

## Neutron Polarization Induced by Radio Frequency Radiation

U. Schmidt,<sup>1</sup> H. Abele,<sup>1</sup> A. Boucher,<sup>1</sup> M. Klein,<sup>1</sup> C. Stellmach,<sup>1</sup> and P. Geltenbort<sup>2</sup>

<sup>1</sup>*Physikalisches Institut der Universität Heidelberg, 69120 Heidelberg, Germany*

<sup>2</sup>*Institut Laue-Langevin, B.P. 156, F-38042 Grenoble Cedex 9, France*

(Received 14 May 1999)

We have measured that an unpolarized ultracold neutron beam gets polarized through its interaction with a resonant radio frequency field. Both spin components pass through the field and end up in one single spin state. We present a simple description for this surprising effect together with first experimental results.

PACS numbers: 29.27.Hj, 33.55.Be, 39.20.+q, 67.65.+z

In 1981 the first observation of the neutron kinetic energy shift due to magnetic resonance was reported by Alefeld *et al.* [1]. Meanwhile in beam neutron magnetic resonance has become a wide field of investigations and applications [1–3]. Also a scheme of dynamical polarization of neutrons was proposed by Badurek *et al.* [2], but never realized. Within their scheme, in beam magnetic resonance is used to obtain a spin dependent kinetic energy shift. In a following static field region the differences in the accumulated Larmor phase of the two spin states due to the kinetic energy shift lead to polarization. They neglect the longitudinal Stern-Gerlach effect inside the magnetic resonance region, which as we point out in the following can be used to obtain polarization without the need of an additional magnetic field downstream of the beam. In this Letter we report the observation of a beam polarization introduced by the interaction of ultracold neutrons with an electromagnetic resonance field, opening the way to a new technique for neutron polarization without the use of material or matter in the beam. Instead of removing the unwanted spin state, we apply a radio frequency field to enhance one neutron spin state, by selectively flipping the other spin state.

For ultracold neutrons (UCN) the Zeeman energy in a magnetic field of 1 T is of the same order of magnitude as their kinetic energy. Therefore their kinetic energy changes considerably while traveling into a strong magnetic field.

Assume an in beam NMR experiment with an unpolarized monochromatic UCN beam. An unpolarized UCN beam consists of an incoherent mixture of 50% spin up and 50% spin down particles. The spin component of an UCN parallel to the static NMR field (spin up) is slowed down while traveling into the strong magnetic field region due to the longitudinal Stern-Gerlach effect. In contrast, its spin down component is accelerated and therefore the traveling time through the magnetic field region is shorter than for the spin up component. Inside the static magnetic field we apply a perpendicular rf field, tuned to resonance with the Larmor precession of the UCN spin in the static field. The phase of the Rabi oscillation due to the rf field is proportional to the traveling time through the rf field and to its strength. As a consequence the Rabi phase for both spin components is different as well as the

probability of a spin flip. By carefully tuning the strength of the static and the rf field we can achieve an inversion of an initial spin up UCN and none for an initial spin down UCN. Both initial spin states thus exit the NMR region pointing up. In this way we obtain a totally polarized UCN beam *without filtering out* one of the initial spin states.

Figure 1 shows schematically the transitions of the two possible initial states of a monochromatic UCN beam to the four possible final states after passing a resonant rf field inside a static magnetic field. Inside the static magnetic field  $B_0$  the potential energy of an UCN with spin up is  $E_M/2$ , for an UCN with spin down  $-E_M/2$ , with  $E_M = \hbar\gamma B_0$  (gyromagnetic ratio of neutrons  $\gamma = 183.25$  MHz/T). Because the total energy of the UCNs is conserved, the change of the kinetic energy of the UCN is the same as the change of the potential energy, but with opposite sign. The probability of a spin flip due to the resonant rf field  $B_{rf}$  follows from the Bloch equations for a spin 1/2 particle:  $P(\text{spin flip}) = \sin^2(\omega_R/2\tau)$ . The Rabi phase  $\omega_R\tau$  is the Rabi frequency  $\omega_R = \gamma B_{rf}$  times the time of flight  $\tau$  through the rf field  $B_{rf}$ . Writing the Rabi phase in terms of the initial kinetic energy  $E_{k0}$  and the kinetic energy inside the static  $B_0$  field  $E_{kin}$  leads to the following expression:

$$\omega_R\tau = \gamma B_{rf} \frac{L}{v} = \gamma B_{rf} L \sqrt{\frac{m}{2E_{kin}}} = \frac{\Phi_0}{\sqrt{E_{kin}/E_{k0}}}, \quad (1)$$

$$\Phi_0 = \gamma B_{rf} L \sqrt{\frac{m}{2E_{k0}}}.$$

$L$  denotes the length of the flight path,  $v$  the velocity, and  $m$  the mass of the UCNs. More general, for arbitrary shapes of the rf field, the  $B_{rf}L$  term in the expression for  $\Phi_0$  must be replaced by the rf field integral along the flight path of the UCN. Inserting the kinetic energy inside the  $B_0$  field for the two initial spin states leads to the scheme shown in Fig. 1. For the Rabi phases we write

$$\begin{aligned} \text{initial spin up (}\uparrow\text{): } \Phi^+ &= \frac{\Phi_0}{\sqrt{1 - E_M/2E_{k0}}}, \\ \text{initial spin down (}\downarrow\text{): } \Phi^- &= \frac{\Phi_0}{\sqrt{1 + E_M/2E_{k0}}}. \end{aligned} \quad (2)$$

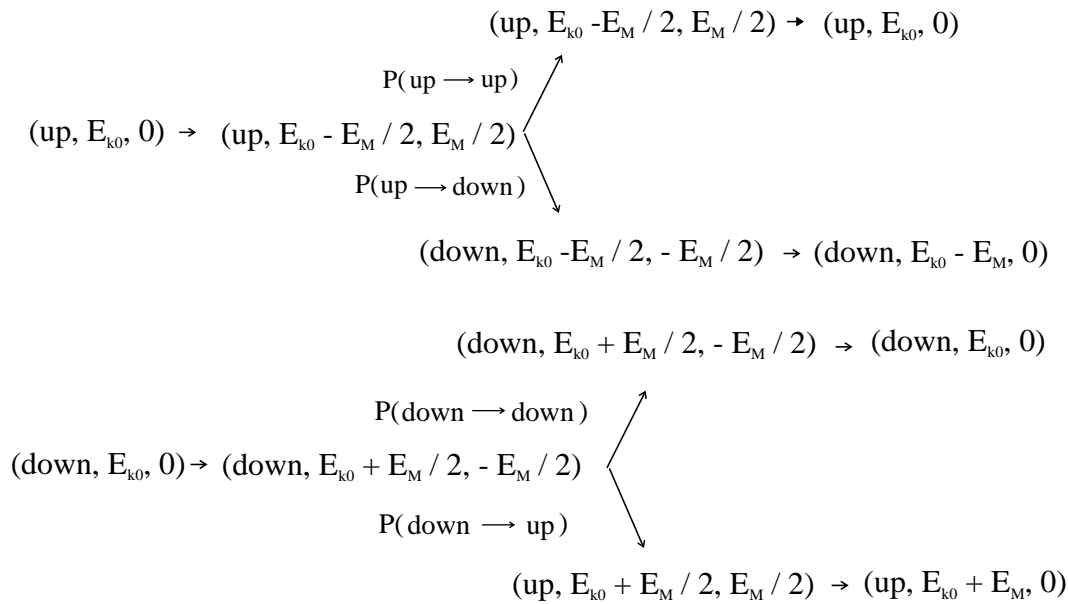


FIG. 1. Schematic representation of the spin state, the kinetic energy (second value), and the potential energy (third value inside the brackets) of UCNs passing through a resonant rf field inside a static magnetic field.

The probabilities for the spin transitions originated by the Rabi oscillations are

$$\begin{aligned}
 P(\uparrow \rightarrow \uparrow) &= \cos^2 \frac{\Phi^+}{2}, \quad \text{for } E_M < 2E_{k0}, \\
 P(\downarrow \rightarrow \downarrow) &= \cos^2 \frac{\Phi^-}{2}, \\
 P(\uparrow \rightarrow \downarrow) &= \sin^2 \frac{\Phi^+}{2}, \quad \text{for } E_M < E_{k0}, \\
 P(\downarrow \rightarrow \uparrow) &= \sin^2 \frac{\Phi^-}{2}.
 \end{aligned} \tag{3}$$

For a magnetic energy higher than the limits given in Eqs. (3), a spin up UCN is reflected and cannot pass

through the magnetic field region. The induced emission of a photon of the rf field is described by the transition up  $\rightarrow$  down, which changes the potential energy of the UCN from  $E_M/2$  to  $-E_M/2$ . The induced absorption of a photon is given by the transition down  $\rightarrow$  up. After passage of the rf field region the potential energy is converted into kinetic energy of the neutron due to the gradient of the  $B_0$  field. We end up with the final states shown in Fig. 1. The polarization  $\langle \sigma_z \rangle$  of an UCN beam then is the relative difference of the population of the two spin states. For an initially unpolarized UCN beam, for which half of the neutrons are in the spin up state and half are in the spin down state, the polarization after passage of a resonant rf field follows from (3):

$$\begin{aligned}
 \langle \sigma_z \rangle &= \frac{1}{2} \left( \cos^2 \frac{\Phi^+}{2} - \sin^2 \frac{\Phi^+}{2} \right) - \frac{1}{2} \left( \cos^2 \frac{\Phi^-}{2} - \sin^2 \frac{\Phi^-}{2} \right) = \frac{1}{2} (\cos \Phi^+ - \cos \Phi^-), \quad \text{for } E_M \leq E_{k0}, \\
 \langle \sigma_z \rangle &= \frac{\cos^2 \frac{\Phi^+}{2} + \sin^2 \frac{\Phi^-}{2} - \cos^2 \frac{\Phi^-}{2}}{\cos^2 \frac{\Phi^+}{2} + \sin^2 \frac{\Phi^-}{2} + \cos^2 \frac{\Phi^-}{2}} = \frac{1 + \cos \Phi^+ - 2 \cos \Phi^-}{3 + \cos \Phi^+}, \quad \text{for } E_{k0} < E_M < 2E_{k0}, \\
 \langle \sigma_z \rangle &= \sin^2 \frac{\Phi^-}{2} - \cos^2 \frac{\Phi^-}{2} = -\cos \Phi^-, \quad \text{for } E_M \geq 2E_{k0}.
 \end{aligned} \tag{4}$$

For  $E_M \geq 2E_{k0}$  UCNs with initial spin up are reflected by the magnetic potential of the  $B_0$  field. Therefore the polarization of the UCNs after the magnetic fields is the same as in the case of an initial beam with polarization  $-1$ . In this case the intensity of the final beam is half of the intensity of the initial unpolarized beam. In the case of  $E_{k0} < E_M < 2E_{k0}$  only the UCNs which undergo the transition up  $\rightarrow$  down are reflected. As a consequence we obtain the full intensity of UCNs in the final beam if the polarization is 1, but only half of the intensity if the polarization is  $-1$ . For  $E_M < E_{k0}$  all UCNs pass the magnetic fields and we have always the full intensity,

independent of the final polarization. Minima and maxima of the polarization are found for

$$\begin{aligned}
 \Phi^+ &= n\pi; & \Phi^- &= m\pi; & n > m; & n, m \in N \\
 & & & & & \text{for } E_M < 2E_{k0},
 \end{aligned}$$

in particular,

$$\begin{aligned}
 \langle \sigma_z \rangle &= 1 \quad \text{for } n = \text{even}, m = \text{odd}, \\
 \langle \sigma_z \rangle &= -1 \quad \text{for } n = \text{odd}, m = \text{even}, \\
 \langle \sigma_z \rangle &= 0(\text{saddle point}) \quad \text{for } n, m = \text{even or } m, n = \text{odd}.
 \end{aligned}$$

For given natural numbers  $n$  and  $m$  ( $n > m$ ) we calculate  $\Phi_0$  and  $E_M$  at this point to

$$E_M = \frac{n^2 - m^2}{n^2 + m^2} 2E_{k0}; \quad \Phi_0 = n\pi \sqrt{\frac{2m^2}{n^2 + m^2}}. \quad (5)$$

Figure 2 shows the expected polarization of the final UCN beam in dependence of the magnetic energy  $E_M/E_{k0} \propto \mu B_0$  and  $\Phi_0/2\pi \propto B_{rf}$ .

The experiment was done at the UCN test beam facility of the UCN turbine (PF2) at the high flux reactor of the Institut Laue Langevin (ILL) at Grenoble (France). Figure 3 shows a sketch of the experimental setup. For the wavelength selection of the UCN we used a storage volume with an absorbing top [4] (Fig. 3 energy selector). UCNs with insufficient kinetic energy could not reach the bottom of the storage volume against the Earth's gravitational field, while UCNs with too high kinetic energy hit the top and were absorbed. The bottom of the storage volume was mounted 1.41 m and the top 1.79 m above the horizontal beam axis.

The component of the UCN velocity along the beam axis determines the traveling time through the rf field. We measured the corresponding de Broglie wavelength spectrum with a time of flight setup using a beam chopper. The deconvolution of a measured time of flight spectrum with the time resolution of the chopper shows a spectrum with a maximum at 66 nm wavelength and a FWHM of 12%. A tail of long wavelengths due to the beam divergency up to  $40^\circ$  causes the mean wavelength to be 69.6 nm. Additionally we had a small contribution of shorter wavelengths, because we operated the energy selector in the continuous mode in order to gain intensity. The measured spectrum was in good agreement with theoretical calculations.

The  $B_0$  field was generated by a superconducting solenoid (30 cm long, 8 cm inner diameter, 13 cm outer diameter) with a relative field inhomogeneity  $1 \times 10^{-3}$  across the rf field region. The ratio between the rf field, needed for a  $\pi$  spin flip, and a  $B_0$  field of 1 T is  $1 \times 10^{-4}$ . This value corresponds to the maximum tolerable  $B_0$  field

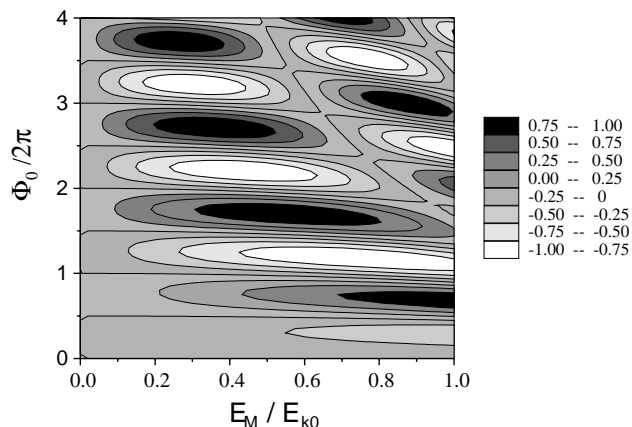


FIG. 2. Expected polarization of an initially unpolarized UCN beam after passing a resonant rf field.

inhomogeneity, in order to be in resonance. With a pair of compensation coils in a split pair configuration the inhomogeneity of the  $B_0$  field decreased to  $1.2 \times 10^{-4}$  (result of a fit of a measured resonance curve).

Eight little coils of five windings each, arranged like the spokes of a wheel, generate a ring shaped rf field perpendicular to the longitudinal  $B_0$  field. The support of these coils has windows between the coils for the UCNs, because of poor penetration of UCNs through matter. The variance of the rf field integral  $\int_L B_{rf} dl$  along different flight paths of UCNs through these windows is  $\sigma(\int_L B_{rf} dl) / (\int_L B_{rf} dl) = 0.1$ . We get this value from a Monte Carlo calculation.

We determined the degree of polarization with a fast adiabatic spin flipper [5] in combination with a polarization foil [6]. The spins of the UCNs turned adiabatically from the longitudinal direction of the  $B_0$  field to the transversal direction of the static field of the fast adiabatic spin flipper due to the superposition of both fields in the region between the two devices. The polarization foil was magnetized in a strong magnetic field transversal to the beam axis and consists of an aluminum foil covered with a  $1 \mu\text{m}$  thick FeCo layer. Only spin down UCNs could penetrate the foil, because of the high magnetic potential inside the FeCo layer. The cutoff of the polarization foil for long wavelengths was measured to be 95 nm for spin down UCNs.

The chopper for the time of flight measurement has an open to close ratio of 0.1 and was operated with 5 Hz rotation frequency. The length of the flight path between the chopper and the active volume of the detector was 48 cm. The UCN detection was done with a microstrip detector [7] loaded with a partial pressure of 50 mbar of  $^3\text{He}$ . Having fixed the beam chopper in the open position, the counting rate of the UCNs was 290 counts in 300 s.

With the rf field switched on, we measured a resonance curve by ramping the  $B_0$  field strength. A fit to this resonance curve results in a resonance frequency of  $\nu_{\text{res}} = 23.4932$  MHz which corresponds to a  $B_0$  field of 0.80553 T. With  $\bar{\lambda} = 69.6$  nm follows  $E_M/E_{k0} = 0.576$ . At the resonance frequency we varied the rf field amplitude (see Fig. 4). Without the use of the spin flipper only spin down UCNs can pass through the polarizer foil and reach the detector. For initial spin up UCNs which are

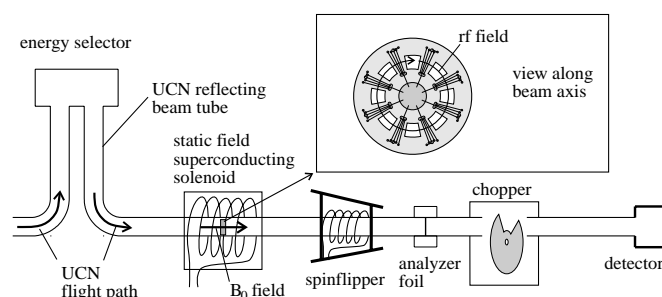


FIG. 3. Sketch of the experimental setup as installed at the ILL PF2-facility.

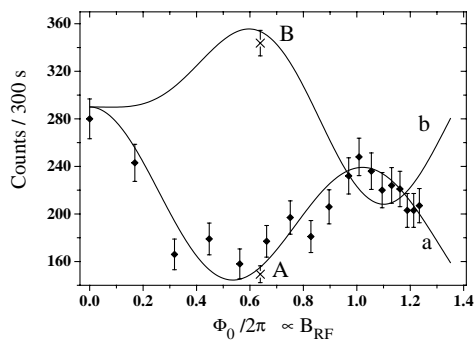


FIG. 4. Rabi oscillation of initially unpolarized UCNs; curve *a*: without spin flipper; curve *b*: with spin flipper. (Through going lines are theoretical calculations; see text.)

flipped by induced emission of a photon the wavelength  $\bar{\lambda} = 69.6$  nm is shifted to  $\bar{\lambda} = 107$  nm. This is above the cutoff of the polarizer and these UCNs cannot reach the detector. Therefore the counting rate behaves like a cosine function equal to the case when we start with an initial polarization of  $-1$ . Averaging over the spectrum and the rf field integral and the  $B_0$  field for different flight paths of the UCNs results in curve *a* of Fig. 4. Additionally, a loss of polarization of 10% due to nonperfect magnetic orientation inside the polarizer foil is included in the calculation. This depolarization was separately measured. Switching the spin flipper on at a rf field of point A of Fig. 4 shows the counting rate of point B. The polarization of the UCNs derived from point A and B is  $(39.4 \pm 2.4)\%$ . Because only unflipped spin up UCNs can reach the detector, the polarization shows the same dependence on  $\Phi_0 \propto B_{rf}$  as in the case of  $E_{k0} < E_M < 2E_{k0}$  [see Eq. (4)]. Compared to a normal spin filtering polarizer we get an intensity gain factor of 1.2. Figure 5 (data, with  $B_{rf}$ ) shows the UCN wavelength spectrum at point B (Fig. 4).

An initially spin down UCN, which was flipped by induced absorption of a photon (curve *b*, Fig. 5), has a shorter wavelength as an unflipped spin up UCN (curve *a*, Fig. 5). Therefore they can penetrate the polarizer foil after an additional spin flip due to the spin flipper. The data are in good agreement with the calculated spectrum (curve *c*, Fig. 5). To demonstrate the effect of the wavelength shift we measured a spectrum without a rf field (Fig. 5, data, without  $B_{rf}$ ). In this case only initially spin up UCNs reach the detector (curve *a*, Fig. 5). The width of the shown spectra is mainly originated in the poor time resolution of the chopper.

In conclusion, we find that an unpolarized UCN beam becomes polarized while interacting with a resonant rf field. Our experiments demonstrate clearly this effect. Additionally we observed the energy shift of UCNs caused by an absorption of a rf photon. Because of the kinetic

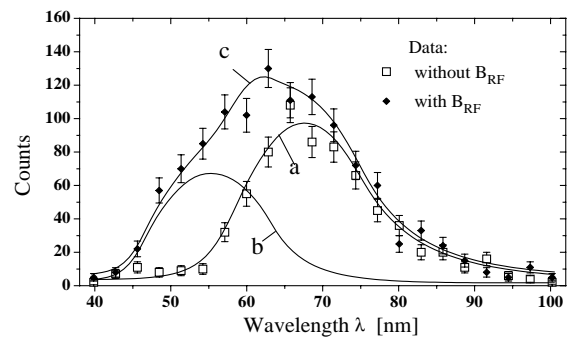


FIG. 5. Spectra of final spin up UCNs (spin flipper switched on). Curve *a*: Calculated spectrum of initial spin up UCNs. Curve *b*: Calculated spectrum of flipped initial spin down UCNs (flip efficiency derived from data of Fig. 4 is included). Their wavelengths are shifted due to induced absorption of a photon. Curve *c*: Sum of *a* and *b*.

energy shift of one of the initial spin states, the phase space density is conserved and also Liouville's theorem. Taking the efficiency 0.9 of our polarization analysis into account we reached a polarization of 44% and a gain factor of 1.2 in intensity compared to a conventional UCN polarizer. The polarization and the gain factor for intensity were limited in our experiment by the homogeneity of our  $B_0$  field of  $1.2 \times 10^{-4}$ . For a homogeneity of  $10^{-5}$ , calculation shows a polarization of 88%. The gain factor will be nearly the same as in our experiment for the same  $E_M/E_{k0} = 0.58$ . But for  $E_M/E_{k0} = 1.2$  the gain factor increases to 1.7 and the polarization to 92%. To reach a homogeneity of the  $B_0$  field of  $10^{-5}$  does not take much effort, but was out of the scope of our first experimental approach.

This work has been funded by the German Federal Minister for Research and Technology (BMFT) under Contract No. 06HD854I. We thank the staff of the ILL research reactor, especially H. Just for support and D. Dubbers for helpful discussions.

- [1] B. Alefeld, G. Badurek, and H. Rauch, *Z. Phys. B* **41**, 231 (1981).
- [2] G. Badurek, H. Rauch, and A. Zeilinger, *Z. Phys. B* **38**, 303 (1980).
- [3] R. Golub, R. Gähler, and T. Keller, *Am. J. Phys.* **62**, 779 (1994).
- [4] R. Golub, D.J. Richardson, and S.K. Lamoreaux, *Ultra Cold Neutrons* (Hilger, Bristol, 1991).
- [5] A. I. Egorov, V. M. Lobashev, V. A. Nazarenko, G. D. Porsev, and A. P. Serebrov, *Sov. J. Nucl. Phys.* **19**, 147 (1974).
- [6] R. Herdin, A. Steyerl, A. R. Taylor, J. M. Pendelbury, and R. Golub, *Nucl. Instrum. Methods* **148**, 353 (1978).
- [7] A. Oed, *Nucl. Instrum. Methods Phys. Res., Sect. A* **263**, 351 (1988).